Stern, E. A., Bunker, B. A., & Heald, S. M. (1980) *Phys. Rev. B: Condens Matter 21*, 5521–5539.
Stricks, W., & Kolthoff, I. M. (1951) *J. Am. Chem. Soc. 73*, 1723–1727.
Teo, B.-K., Lee, P. A., Simons, A. L., Eisenberger, P., & Kincaid, B. M. (1977) *J. Am. Chem. Soc. 99*, 3854–3856.
Twedt, D. C., Sternleib, I., & Gilbertson, S. R. (1979) *J. Am. Vet. Med. Assoc. 175*, 269–275.
Vasak, M., & Kägi, J. H. R. (1983) *Met Ion Biol. Syst. 15*, 213–273.
Vasak, M., Hawkes, G. E., Nicholson, J. K., & Sadler, P. J. (1985) *Biochemistry 24*, 740–747.
Vortisch, V., Kroneck, P., & Hemmerich, P. (1976) *J. Am. Chem. Soc. 98*, 2821–2826.
Vranka, R. G., & Amma, E. L. (1966) *J. Am. Chem. Soc. 88*, 4270–4271.
Wasson, J. R., Mitchell, T. P., & Bernard, W. H. (1968) *J. Inorg. Nucl. Chem. 30*, 2865–2866.
Weser, U., Hartmann, H.-J., Fretzdorff, A., & Strobel, G.-J. (1977) *Biochim. Biophys. Acta 493*, 465–477.
Winge, D. R., Premakumar, R., & Rajagopalan, K. V. (1975) *Arch. Biochem. Biophys. 170*, 242–252.
Winge, D. R., Geller, B. L., & Garvey, J. (1981) *Arch. Biochem. Biophys. 208*, 160–166.
Woolery, G. L., Powers, L., Peisach, J., & Spiro, T. G. (1984a) *Biochemistry 23*, 3428–3434.
Woolery, G. L., Powers, L., Winkler, M., Solomon, E. I., & Spiro, T. G. (1984b) *J. Am. Chem. Soc. 106*, 86–92.

Secondary Structure in Sea Anemone Polypeptides: A Proton Nuclear Magnetic Resonance Study†

Paul R. Gooley and Raymond S. Norton*
School of Biochemistry, University of New South Wales, Kensington 2033, Australia
Received October 10, 1985

ABSTRACT: Elements of secondary structure in the sea anemone polypeptides anthopleurin A and *Anemonia sulcata* toxin I have been defined with the following nuclear magnetic resonance (NMR) spectroscopic data: the pattern of nuclear Overhauser enhancement (NOE) connectivities observed in two-dimensional NMR spectra for protons along the polypeptide backbone, NOE's between protons on separate strands of the polypeptide backbone, peptide NH exchange rates, and NH–H^{α} spin–spin coupling constants. These two polypeptides contain a region of four short strands of antiparallel β-sheet but little or no α-helix. This region of β-sheet brings the aromatic rings of Trp-23 and -33 into close proximity to form the nucleus for a small hydrophobic region. A type II reverse turn involving residues 30–33 has also been defined. Our results are compared with previous predictions of the secondary structure of these polypeptides. The structures are also discussed in relation to that of a scorpion toxin that appears to bind to a similar site on the sodium channel of excitable tissue.

Sea anemones contain a series of polypeptides of molecular weight about 5000, which exert potent effects on excitable tissue. One of these polypeptides, anthopleurin A (AP-A),[1] isolated from the northern Pacific species *Anthopleura xanthogrammica* (Norton, 1981; Norton et al., 1978), exerts a selective, potent, positive inotropic effect on the mammalian heart, without affecting heart rate or blood pressure (Shibata et al., 1976; Blair et al., 1978). AP-A is more potent and has a higher therapeutic index in vivo (Scriabine et al., 1979) than the cardiac glycoside digoxin. Its activity appears to be due to a specific interaction with the sodium channel of cardiac tissue, which leads to a delay in inactivation of the channel and thus a lengthening of the action potential and a greater influx of sodium ions (Kodama et al., 1981).

Other members of this homologous series of polypeptides for which amino acid sequences have been determined include anthopleurin C (Norton, 1981; Norton et al., 1978) from the anemone *Anthopleura elegantissima* and toxins I (Wunderer & Eulitz, 1978), II (Wunderer et al., 1976), and V (Scheffler et al., 1982) from the Mediterranean species *Anemonia sulcata*. The most thoroughly investigated of these is *Anemonia sulcata* toxin II (ATX II), which acts on the mammalian heart (Ravens, 1976) and on various nerve preparations (Bergman et al., 1976; Romey et al., 1976) by the same mechanism as AP-A, that is, by delaying inactivation of the sodium channel. Indeed, a considerable effort has been devoted to characterizing the mechanisms of action of these polypeptides (Beress, 1982; Alsen, 1983). By contrast, very little detailed information is available on their structures in solution. AP-A has been investigated by laser Raman, circular dichroism, and fluorescence spectroscopy (Ishizaki et al., 1979), as well as by natural abundance ^{13}C NMR spectroscopy (Norton & Norton, 1979, 1980; Norton et al., 1982). ATX II has been the subject of laser Raman (Prescott et al., 1976) and ^{13}C NMR (Norton et al., 1980) spectroscopic studies. While some information about the overall strutures of these molecules, as well as the local environments of specific residues, has emerged from these investigations, a detailed picture of their structures in solution

† Financial support by the Australian Research Grants Scheme is gratefully acknowledged.
* Address correspondence to this author.

[1] Abbreviations: AP-A, anthopleurin A; ATX I, *Anemonia sulcata* toxin I; ATX II, *Anemonia sulcata* toxin II; DSS, sodium 4,4-dimethyl-4-silapentane-1-sulfonate; NOE, nuclear Overhauser enhancement; COSY, two-dimensional homonuclear correlated spectroscopy; NOESY, two-dimensional homonuclear dipolar exchange spectroscopy.

0006-2960/86/0425-2349$01.50/0

is not yet available. We have therefore undertaken a study of this series of molecules by high-resolution ^1H NMR spectroscopy.

Previously, we reported the results of a ^1H NMR study on ATX I in which a number of resonances were assigned and the effects of pH and temperature investigated (Gooley et al., 1984a). A preliminary study of AP-A and ATX II showed that each exhibited heterogeneity in solution, which may be due to the presence of cis and trans conformers around the Gly-40 to Pro-41 peptide bond (Gooley et al., 1984b). More recently, we have specifically assigned a large number of resonances in the ^1H NMR spectra of AP-A and ATX I (Gooley et al., 1985; Gooley & Norton, 1985a,b). This paper describes aspects of the secondary structure of these two polypeptides, which can be deduced from these assignments and from additional NMR data presented herein.

Materials and Methods

Materials. AP-A was isolated from *Anthopleura xanthogrammica* by the methods of Norton et al. (1978) or Schweitz et al. (1981) and ATX I and II from *Anemonia sulcata* by the method of Beress et al. (1975). During the course of the NMR experiments, the samples were periodically subjected to chromatography on Sephadex G-50 in 0.1 M NaCl at pH 3, followed by Sephadex G-10 in 1 mM HCl or distilled water, in order to avoid contamination by aggregated polypeptide or paramagnetic impurities. ^2H_2O (≥99.75% ^2H) was obtained from the Australian Atomic Energy Commission, Lucas Heights, NSW. pH values of samples for NMR experiments were measured at 22 °C with an Activon Model 101 pH meter and Ingold 6030-02 (or -04) microelectrode. Reported values are meter readings uncorrected for deuterium isotope effects.

NMR Spectroscopy. ^1H NMR spectra were recorded at 300.07 MHz on a Bruker CXP-300 spectrometer operating in the pulsed Fourier-transform mode with quadrature detection. Spinning sample tubes of 5-mm o.d. (Wilmad Glass Co., 527-PP grade) were used, and the probe temperature was maintained with a Bruker B-VT 1000 variable-temperature unit. Chemical shifts are expressed in ppm downfield from DSS but were measured with a trace of internal dioxane at 3.751 ppm downfield from DSS. Taking into account data from two-dimensional spectra, their estimated accuracy is ±0.02 ppm.

Two-dimensional homonuclear correlated (COSY) spectra were recorded with the pulse sequence (Aue et al., 1976)

$$(t_0\text{–}90°\text{–}t_1\text{–}90°\text{–}t_2)_n$$

where t_1 and t_2 are the evolution and observation periods, respectively. Spectra were recorded with 255 (or 511) increments of t_1 from 0.01 to 67 (or 134) ms, t_2 = 0.27 s, and spectral width of 3788 Hz. Data were acquired in 2048 points at each t_1 value. The carrier was placed in the center of the spectrum, and quadrature detection was employed in both dimensions, with appropriate phase cycling to select *N*-type peaks. NOESY spectra were recorded with the pulse sequence (Jeener et al., 1979)

$$(t_0\text{–}90°\text{–}t_1\text{–}90°\text{–}\tau_M\text{–}90°\text{–}t_2)_n$$

where τ_M is the mixing time. A total of 256 t_1 values ranging from 0.01 to 33.8 ms were accumulated, with τ_M = 200 ms, t_2 = 0.14 s, and spectral width of 7576 Hz. To suppress contributions from coherent magnetization, the mixing time was randomly varied by ±5% for various t_1 values. Data were acquired in 2048 points at each t_1 value. The carrier was placed at the low-field end of the spectrum, and appropriate phase cycling used to eliminate experimental artifacts. In all two-dimensional spectra, low-power irradiation of the water resonances was applied continuously during the period t_0 (typically 1.5 s) and in NOESY experiments also during τ_M.

Prior to Fourier transformation, two-dimensional NMR spectra were multiplied in the t_1 and t_2 dimensions by a sine-bell window function and then zero-filled to 1024 points in t_1 and 4096 points in t_2 in the case of COSY spectra and 2048 points in t_1 and 4096 points in t_2 for NOESY spectra. All spectra are shown in the absolute value mode without symmetrization.

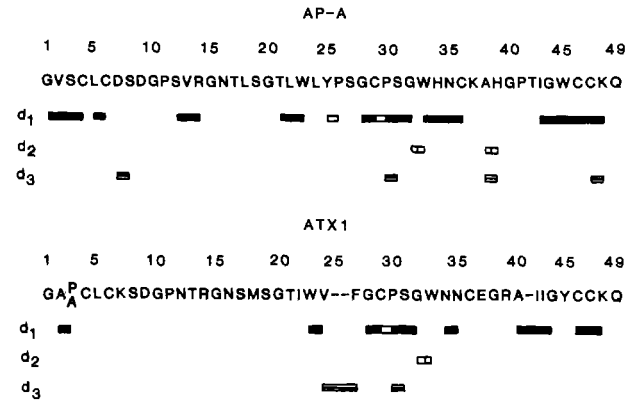

FIGURE 1: Amino acid sequences of AP-A and ATX I and summary of NOESY connectivities used for sequential assignment of resonances: (■) sequential assignment via d_1 (H_i^α to NH_{i+1}); (▥) sequential assignment via d_2 (NH_i to NH_{i+1}); (▤) sequential assignment via d_3 (H_i^β to NH_{i+1}); (□) sequential assignment via NOE's from H_i^α to Pro H_{i+1}^δ.

Results and Discussion

Specific Assignment of Resonances. Recently, we have assigned a large number of resonances in the ^1H NMR spectra of AP-A and ATX I to specific resides in the sequence (Gooley et al., 1985; Gooley & Norton, 1985a,b). Many of these resonance assignments have been made by the technique of sequential assignments (Billeter et al., 1982; Wüthrich, 1983) in which through-bond (COSY) connectivities are used to link each peptide NH to its corresponding H^α and, thus, to a defined spin system from the side chain, together with through-space (NOESY) connectivities, which link each NH to one or more protons from a neighboring residue in the amino acid sequence. The three most useful distances [using the nomenclature of Billeter et al. (1982)] are d_1, from H_i^α to NH_{i+1}, d_2, from NH_i to NH_{i+1}, and d_3, from H_i^β to NH_{i+1}. These distances depend on the peptide backbone dihedral angles ϕ_i and ψ_i, as well as the side-chain angle χ^1_i.

Those residues of AP-A and ATX I whose resonances have been specifically assigned on the basis of the distances d_1, d_2, and d_3 are indicated in Figure 1. Assignments are incomplete for both polypeptides. Of the 48 residue pairs in AP-A, 19 are assigned by d_1 connectivities and 2 by d_2 connectivities. Taking account of the four Pro residues in AP-A, this leaves 22 pairs for which neither d_1 nor d_2 connectivities have been identified. In ATX I this figure is somewhat higher. Possible reasons why d_1 or d_2 connectivities may not have been observed for all of the residues in AP-A or ATX I have been outlined previously (Gooley & Norton, 1985a,b). Conformational averaging, which may be important in some regions of the polypeptide backbone, can also lead to a reduction in NOE values amongst the backbone protons. In both polypeptides, several additional residues have been assigned by other means, for example, by sequence homology. However, it is the residues for which d_1 and d_2 connectivities are available that can be most readily defined in terms of their secondary structure.

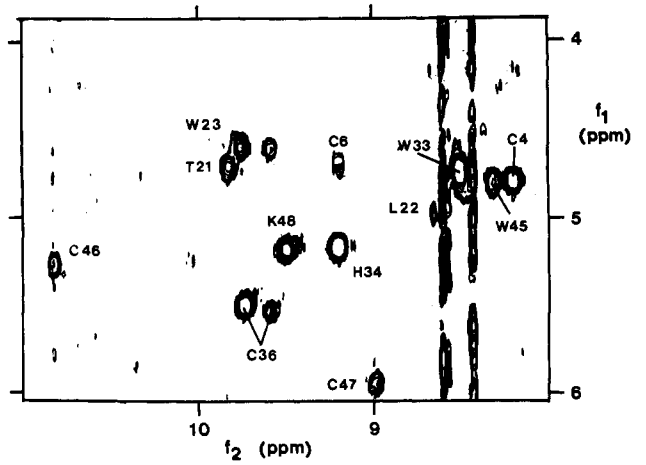

FIGURE 2: Contour plot of the spectral region f_1 = 3.9–6.05 ppm and f_2 = 8.0–11.05 ppm of a 300-MHz ^{1}H COSY spectrum of 16 mM AP-A in ^2H_2O, pH 3.9, 12 °C. Only those backbone NH protons that exchange slowly with solvent give rise to resonances in this region. Resonances of Cys-36 are split due to conformational heterogeneity.

Secondary Structure. The type of NOE connectivity observed between successive backbone protons is related to the backbone conformation (Billeter et al., 1982; Wüthrich et al., 1984; Arseniev et al., 1984). Stretches of β-pleated sheet, parallel or antiparallel, are characterized by short d_1 distances of the order of 2.2–2.4 Å, while α-helices show short d_2 distances of about 2.8 Å and longer d_1 distances of 3.5–3.6 Å. The fact that most of the sequential assignments in AP-A and ATX I have been made by observation of d_1 connectivities (Figure 1) suggests that the major ordered secondary structure in these molecules is β-sheet, with very little α-helix being present. However, Wüthrich et al. (1984) have noted that the observation of d_1 connectivities is a necessary but not sufficient criterion for the identification of β-sheet structures and that additional criteria are desirable. In the remainder of this section, we describe additional evidence that defines the regions of β-sheet structure in AP-A and ATX I.

A distinctive feature of β-sheet structures is that the constituent strands are stabilized by hydrogen bonds between the amide and carbonyl groups of adjacent strands. The amide protons that participate in these hydrogen bonds will exchange slowly with solvent. Figure 2 shows the amide region of a COSY spectrum of fully protonated AP-A dissolved in ^2H_2O at pH 3.9 and 12 °C. Cross peaks from 14 NH protons to their corresponding H^α protons are observed in this spectrum. Thirteen of these are assigned to 12 residues, one of the cross peaks being split due to conformational heterogeneity. The remaining peak is unassigned, and it is not known if it represents the minor form of a split resonance. As indicated in Figure 2, these slowly exchanging NH protons are assigned to amino acid residues occurring in four different segments of the amino acid sequence, 4–6, 21–23, 33–36, and 45–48. Each of these segments is characterized by d_1 connectivities observed in NOESY spectra, consistent with an extended structure such as a β-sheet.

Further definition of this region of β-sheet comes from the observation of NOESY connectivities between these different segments of backbone. In a parallel β-sheet, one expects short $d_1(i,j)$ and $d_2(i,j)$ values, where protons i and j are on different strands. These also occur in an antiparallel β-sheet, but in this structure the α-protons on different strands can also approach one another quite closely. Thus, the observation of NOESY connectivities between H^{α_i} and H^{α_j} serves to distinguish a region of antiparallel β-sheet from a region of parallel β-sheet (Wüthrich et al., 1984).

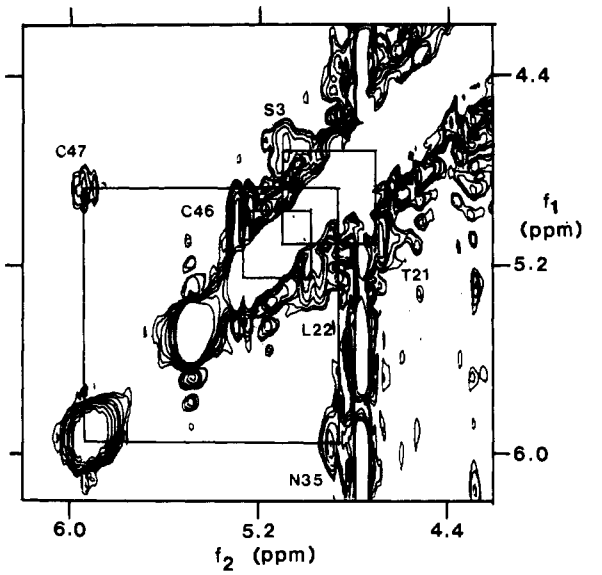

FIGURE 3: Contour plot of the spectral region 4.2–6.2 ppm of a 300-MHz ^{1}H NOESY spectrum of 14 mM AP-A in ^2H_2O, pH 4.7, 27 °C. Connectivities are indicated between pairs of α-protons on different strands of the polypeptide chain.

Figure 3 shows a region of a NOESY spectrum of AP-A in ^2H_2O containing connectivities between the pairs of α-protons from Ser-3 and Thr-21, Leu-22 and Cys-46, and Asn-35 and Cys-47. These NOE connectivities show that these residues form part of a region of antiparallel β-sheet and serve to align the segments relative to one another. This alignment is confirmed by $d_1(i,j)$ NOESY connectivities between Ser-3 and Leu-22 and between Cys-36 and Cys-47 and by $d_2(i,j)$ connectivities between Thr-21 and Cys-47 and between His-34 and Lys-48, as illustrated in the NOESY spectrum of AP-A in ^2H_2O shown in Figure 4.

These observations, encompassing sequential d_1 NOESY connectivities, the location of slowly exchanging backbone amide protons, and interstrand H^α–H^α, $d_1(i,j)$, and $d_2(i,j)$ NOESY connectivities, are summarized in Figure 5. This shows a region of antiparallel β-sheet consisting of four strands of peptide backbone. Trp-33 and Gly-44 are included in this diagram, even though they are not strictly part of the β-sheet, because their α-protons show d_1 connectivities to the NH protons of His-34 and Trp-45, respectively, suggesting that the backbone conformations in these regions continue in the extended conformation typical of a β-sheet.

Further support for this β-sheet structure comes from consideration of backbone NH-H^α spin–spin coupling constants $^3J_{NH-H^\alpha}$. For a β-sheet, these values should be in the range 8–10 Hz (Bystrov, 1976). Measured values for Thr-21, Trp-23, Trp-33, His-34, Cys-36, Trp-45, Cys-46, Cys-47, and Lys-48 all fall within this range. By contrast, $^3J_{NH-H^\alpha}$ for Cys-4 is only 6.5 Hz, suggesting that some distortion of the backbone occurs near this residue, probably as a result of its disulfide linkage to Cys-46.

Gly-1 and Val-2 are not shown in Figure 5 as forming part of this region of antiparallel β-sheet, even though the observation of d_1 NOESY connectivities between Ser-3 and Val-2 and between Val-2 and Gly-1 (Figure 1) is consistent with continuation of an extended backbone conformation to the N-terminus. The NH of Val-2 does not appear in Figure 2, indicating that its rate of exchange with solvent is faster than those of the 14 NH protons visible therein. Thus, if a hydrogen bond exists between NH of Val-2 and the carbonyl of Leu-22, it must be weaker than those indicated in Figure 5. Furthermore, a NOESY connectivity between H^α of Trp-23 and

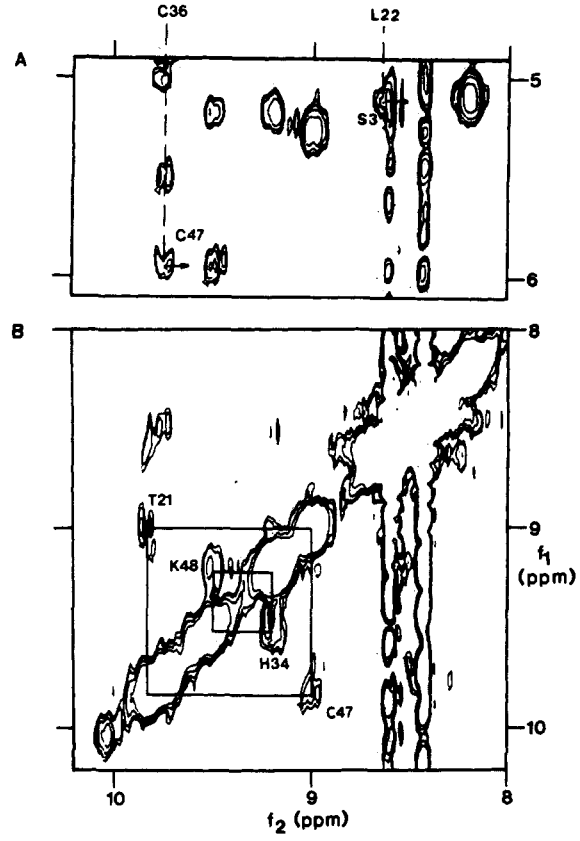

FIGURE 4: Contour plot of the spectral regions (A) f_1 = 4.9–6.1 ppm and f_2 = 8.0–10.2 ppm and (B) $f_1 = f_2$ = 8.0–10.2 ppm of a 300-MHz ^{1}H NOESY spectrum of 14 mM AP-A in ^2H_2O, pH 3.9, 12 °C. Only NH protons that exchange slowly with solvent give rise to cross peaks under these conditions. $d_1(i,j)$ NOE's are indicated in (A) and $d_2(i,j)$ NOE's in (B).

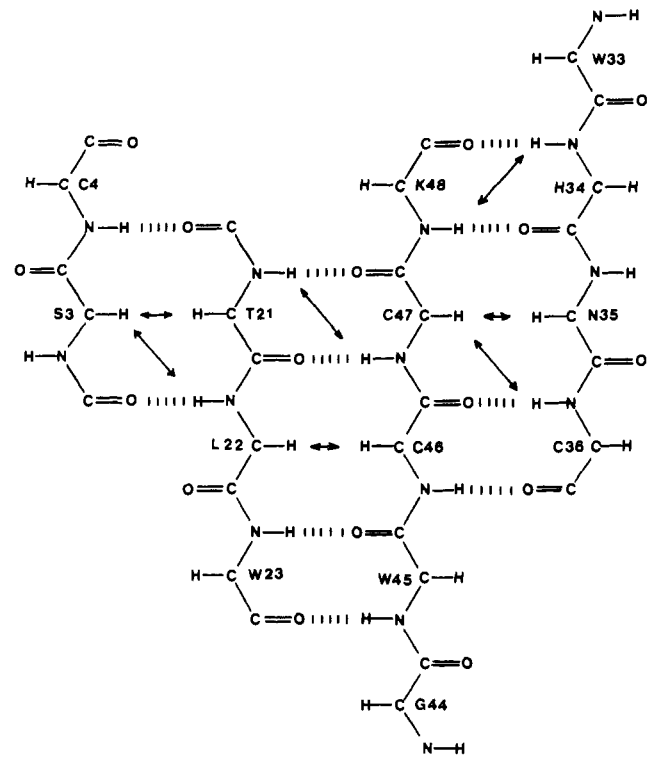

FIGURE 5: Region of antiparallel β-sheet in AP-A. Interstrand NOE's shown in Figures 3 and 4 are indicated by double-headed arrows. Probable hydrogen bonds involving the slowly exchanging backbone NH protons indicated in Figure 2 are also shown.

either of the H^{α}'s of Gly-1 is not observed in our spectra, indicating that the distance between these two α-protons is longer than in the more regular sheet structure shown in Figure 5. Thus, although the peptide backbone from Ser-3 to Gly-1 probably adopts an extended conformation typical of a β-sheet structure, there must be some distortion or flexibility associated with Val-2 and Gly-1.

The evidence described above in support of the region of β-sheet shown in Figure 5 has all been obtained with AP-A. In the case of ATX I, the available data are less complete but are consistent with the presence of a similar structure in this polypeptide. For example, $d_2(i,j)$-type NOESY connectivities are observed between Thr-21 and Cys-47 and Asn-34 and Lys-48, as in AP-A. The NH protons from Thr-21 and Trp-23, Asn-34, Cys-46, Cys-47, and Lys-48 exchange slowly with solvent, consistent with their participation in the hydrogen-bonding network shown for AP-A in Figure 5. There are four other slowly exchanging NH protons in ATX I (at 8.10, 8.53, 8.82, and 8.89 ppm) that have not yet been specifically assigned and that could correspond to some of the remaining hydrogen-bonded NH protons in Figure 5 (for example, the NH resonances of Cys-4, Ile-22, and Cys-36 have not yet been specifically assigned in ATX I). One difference between these regions in ATX I and AP-A occurs at position 45. In AP-A the NH of Trp-45 clearly exchanges slowly with solvent (Figure 2), while in ATX I the NH of Tyr-45 does not, suggesting that the hydrogen bond between NH of Tyr-45 and the carbonyl of Trp-23 (Figure 5) is weak or absent in ATX I.

Another feature of the secondary structure of these polypeptides that is indicated by the NMR data is a type II reverse turn encompassing residues 30–33. Of the three types of reverse turn defined by Venkatachalam (1968), types I and III can be described as a piece of distorted helix (Schulz & Schirmer, 1979). Type II turns are distinguished from types I and III by an approximately 180° rotation of the peptide unit between residues $i + 1$ and $i + 2$. This leads to severe steric hindrance between O_{i+1} and the side chain of residue $i + 2$, such that this type of turn requires Gly at position $i + 2$.

In AP-A the NH resonances of Gly-32 and Trp-33 are sequentially assigned by a strong d_2 NOE (Figure 1). The spin systems of Gly-32 and Trp-33 are linked to those of their other neighboring residues, Ser-31 and His-34, respectively, by d_1 NOE connectivities. As at least four d_2 NOE's are needed to indicate the presence of an α-helix, it appears that the extended chain structure between Ser-31 and His-34 is disrupted between Gly-32 and Trp-33 to form a reverse turn. This turn involves Ser-31 as residue $i + 1$, Gly-32 as $i + 2$, and Trp-33 as $i + 3$. Pro-30 is residue i, which is unusual, as Pro residues usually occupy position $i + 1$. To stabilize the turn, there must be a hydrogen bond between the peptide NH of Trp-33 and the carbonyl of Pro-30. The peptide NH of Trp-33 is one of the slowly exchanging NH's indentified in Figure 2, consistent with its participation in a hydrogen bond. The NH protons of Ser-31 and Gly-32 exchange rapidly with solvent compared to the NH proton of Trp-33.

As the spin systems of Ser-31 and Gly-32 are connected by a d_1 NOE, the reverse turn is of type II (Khaled & Urry, 1976; Wüthrich et al., 1984). If the turn were of type I or type III, a strong d_2 NOE would be observed between the NH protons of Ser-31 and Gly-32 (Wemmer & Kallenbach, 1983; Wüthrich et al., 1984). Even though it is unusual to have Pro as residue i, Gly is always residue $i + 2$ in a type II turn because of steric hindrance. In addition, Trp can only be in the $i + 3$ position of any reverse turn (Schulz & Schirmer,

1979), as observed here. The turn is further characterized by NOE's from H-2 of Trp-33 to H^{β} and H^{α} of Pro-30. These NOE's cannot occur unless there is a turn to bring Pro-30 near Trp-33. In addition, H-2 of Trp-33 shows a NOESY connectivity to its own peptide NH. This NOE, together with other NOE's from Trp-33 to Pro-30, restricts the orientation of the ring of Trp-33 with respect to the reverse turn.

In ATX I a similar pattern of NOESY connectivities is observed for this region of the peptide chain to that described for AP-A, indicating that the same type II reverse turn is also present.

Comparison with Previous Models of Secondary Structure of AP-A and ATX I. The region of antiparallel β-sheet and the reverse turn account for most of the sequential NOESY connectivities indicated in Figure 1 for AP-A. Bearing in mind that the sequential connectivities are incomplete, it is nevertheless worthwhile to compare the conclusions drawn from our NMR data with other evidence on the nature and location of secondary structure elements in AP-A and ATX I. Ishizaki et al. (1979) used the rules of Chou and Fasman (1974) to predict β-reverse turns at the following positions in AP-A (in order of decreasing probability): 20–23, 25–28, 29–32, 7–10, 40–43, and 34–37. β-Sheet regions were predicted for residues 2–6 and 45–49, and no α-helical regions were found. This picture of AP-A as a molecule containing some β-sheet regions, several β-reverse turns, and little or no α-helix was supported by laser Raman and circular dichroism spectroscopic studies carried out by the same authors.

Nabiullin et al. (1982), using the modified Chou–Fasman procedure of Dufton and Hider (1977), predicted that AP-A should have β-sheet regions for residues 16–24 and 38–45, β-turns at positions 10–13, 25–28, and 29–32, and α-helix for residues 2–9 and possibly 33–41. These predictions disagree with those of Ishizaki et al. (1979) with respect to the presence of α-helix and the possible location of β-sheet and of one β-turn. The only point of agreement concerns the existence of β-turns at positions 25–28 and 29–32.

Our NMR data show that neither of these predictions provides an accurate picture of the secondary structure of AP-A. This may be partly due to the presence of three disulfide cross-links in a polypeptide only 49 residues in length. The predictions of Ishizaki et al. (1979) are in better agreement with the NMR data in assigning β-sheet structure to residues 2–6 and 45–49. Nabiullin et al. (1982) predicted β-structure in the region 16–24, which is partially correct (Figure 5). With respect to β-reverse turns, the most probable turn predicted by Ishizaki et al. (1979) is incorrect, as this region forms part of the β-sheet structure (Figure 5). The two groups agree, however, on the presence of reverse turns at positions 25–28 and 29–32. The NMR data show that the latter turn actually encompasses residues 30–33, the slight disagreement possibly being due to the disulfide bond to Cys-29. Our data are incomplete in the region of residues 25–28, but the presence of a reverse turn would be consistent with the β-sheet region shown in Figure 5 and the existence of a type II turn encompassing residues 30–33, as it would provide the means by which the stretch of β-sheet involving residues 21–23 could connect to the turn at positions 30–33 and hence to the subsequent stretch of β-sheet involving residues 33–36. Such an arrangement may also contribute to the proximity of the indole rings of Trp-23 and -33 (see below).

Nabiullin et al. (1982) proposed a model for AP-A based on their secondary structure predictions. The NMR data indicate that this model is incorrect in its inclusion of a region of α-helix near the N-terminus and in the location of β-sheet structures. In addition, a puzzling aspect of this model is that Trp-23 is described as being exposed and Trp-33 and -45 as being buried, the evidence to support this being cited as Ishizaki et al. (1979) and Norton & Norton (1979). We cannot find any evidence to this effect in either of these papers. Indeed, our recent ^{1}H NMR data (Gooley et al., 1985; also see below) show that the indole rings of Trp-23 and -33 are in close proximity to each other and to several other nonpolar side chains, while the indole ring of Trp-45 in AP-A (and indeed the phenolic ring of Tyr-45 in ATX I) is exposed to the solvent.

In the case of ATX I, Nabiullin et al. (1982) predicted that regions 18–27 and 36–43 would form β-sheet, 4–9 an α-helix, and 10–13 and 27–30 β-turns. The NMR data show that there is a stretch of β-sheet within the region 18–27 and a type II reverse turn encompassing residues 30–33 [28–31 using the numbering system for ATX I employed by Nabiullin et al. (1982)]. Thus, there are some points of agreement between the secondary structure predictions and the NMR data for this polypeptide.

Tertiary Structure. Methods for determining the tertiary structure of proteins from NMR data are not as well established as those for the definition of secondary structure. Approaches that have been adopted include the use of NOE data as input for distance–geometry algorithms (Havel et al., 1979; Braun et al., 1981; Williamson et al., 1985) or model building based on elements of secondary structure together with other information such as the location of disulfide cross-bridges (Wemmer & Kallenbach, 1983; Arseniev et al., 1984). Structures obtained by these means can then be refined with energy minimization and/or restrained dynamics simulations (Kaptein et al., 1985).

There are several features of AP-A and ATX I apparent from our NMR data that must be incorporated into a model of their tertiary structures. For example, the indole moieties of Trp-23 and -33 are sufficiently close to one another that their H-7 resonances are linked by NOESY connectivities in both molecules and their aromatic chemical shifts are perturbed by mutual ring current shift interactions (Gooley et al., 1985). Other interactions of Trp-23 and -33, revealed by one- and two-dimensional NOE experiments on AP-A and ATX I, are with H_3^{γ} of Thr-21 (NOE's to H-2 of Trp-23 and H-5/6 of Trp-33), H^{α} and H^{β} of Cys-47 (NOE's to H-2 of Trp-23), and H^{α} of Lys-48 (NOE's to H-4 and H-5/6 of Trp-33). The environment of the indole NH of Trp-23 must be atypical, as its resonance is not observed in one- or two-dimensional spectra recorded with water presaturation, suggesting that it may be in intermediate to fast exchange with solvent. This environment is also preserved in ATX II (Gooley et al., 1985).

The aromatic ring of Trp-33 is also close to the side chain of Pro-30, its H-2 showing NOESY connectivities to H^{β} and H^{γ} of this Pro in both AP-A and ATX I. It is likely that the upfield shifts of nearly 2 ppm for the H^{γ} resonances of Pro-30 (Gooley & Norton, 1985a,b) are due principally to interactions with Trp-33, with possibly some contribution from Tyr-25 in AP-A. Computation of these ring current shifts (Perkins, 1982) for any proposed model of AP-A and ATX I will thus provide a useful check on the local structure of this region.

Of the four Pro residues in AP-A, two, Pro-26 and -30, are preceded by peptide bonds in the trans configuration. The configuration of a third, Pro-11, is not defined by our data. The fourth Pro, at position 41, is also not defined, but it has been suggested previously (Gooley et al., 1984b) that the Gly-40 to Pro-41 peptide bond exists in both the cis and trans

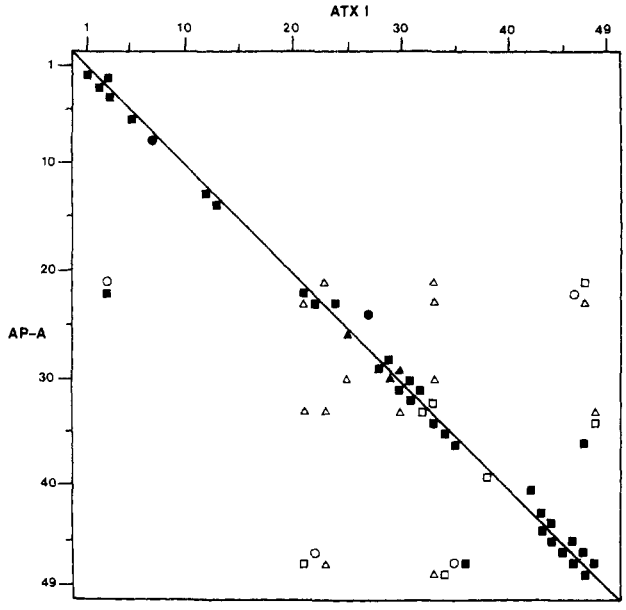

FIGURE 6: Summary of NOESY connectivities between assigned protons in AP-A (lower left triangle) and ATX I (upper right triangle), observed in spectra recorded with a mixing time τ_M of 200 ms. The axes denote the sequences of the polypeptides. Symbols indicate NOE's between proton pairs, as follows: (■) d_1 (H^α to NH); (□) d_2 (NH to NH); (●) d_3 (H^β to NH); (○) $d_{\alpha\alpha}$ (H^α to H^α); (▲) H_i^α to Pro H_{i+1}^δ; (△) NOE's involving side chains.

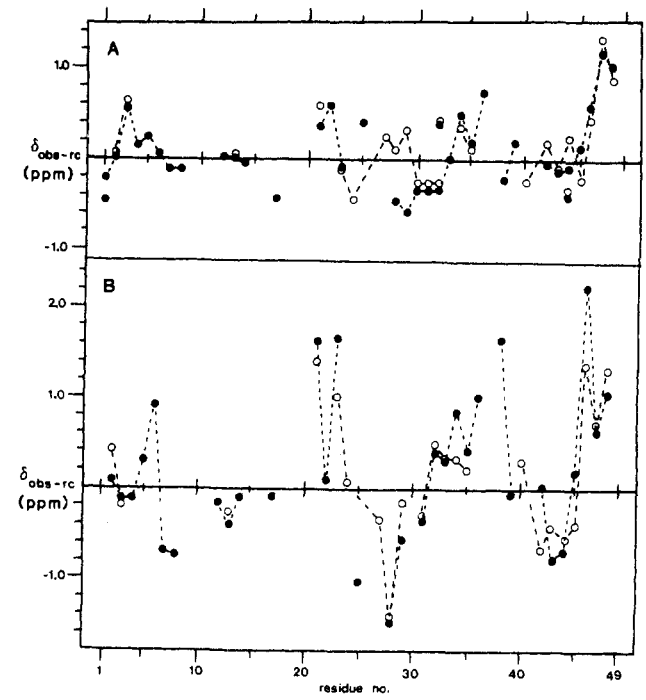

FIGURE 7: Comparison of the differences between observed chemical shifts and random-coil chemical shifts for backbone proton resonances of AP-A (●) and ATX I (○). (A) H^α resonances; (B) NH resonances. Positive values indicate that the proton resonates downfield of its random-coil chemical shift.

configurations in aqueous solution, thus accounting for the conformational heterogeneity observed for AP-A. ATX I lacks Pro-41 and does not display this type of heterogeneity. The peptide chain in the region of the Pro-41 may be part of a loop which is sufficiently flexible to accommodate both isomers. The structural consequences of the cis–trans isomerism, however, extend well beyond the immediate vicinity of this peptide bond, affecting residues as distant in the sequence as Trp-23, which forms part of the region of antiparallel β-sheet shown in Figure 5.

Overall, our data indicate that the gross structures of AP-A and ATX I in solution are similar, although ATX I lacks the major hetereogeneity displayed by AP-A. This similarity is indicated at several points in the preceding discussion but is well illustrated in Figures 6 and 7. Figure 6 is a summary of NOESY connectivities observed for AP-A (lower left triangle) and ATX I (upper right triangle), while Figure 7 summarizes the differences between observed and random-coil chemical shifts for the backbone H^α (Figure 7A) and NH (Figure 7B) resonances of AP-A and ATX I. Although the data for ATX I are less complete, in both figures the similarities between the two sets of data are obvious. In the case of the chemical shifts, the resonances from residues in the antiparallel β-sheet and type II reverse turn in the segments 21–23, 30–36, and 44–48 show striking similarity. In addition, the chemical shifts of residues 2–3 and 42–44, which are at the ends of the β-sheet, are quite similar. The chemical shifts of the H^α resonances of residues 28 and 29 differ, but this may be attributed to the presence of the two extra residues at positions 25 and 26 in AP-A (Figure 1) and/or to Phe-27 in ATX I.

The biological potencies of AP-A and ATX I differ quite markedly, with ATX I being much less active than AP-A on several mammalian nerve and muscle preparations and having a much higher LD_{50} in mice (Norton, 1981; Beress, 1982; Alsen, 1983; Schweitz et al., 1981). At the level of structural detail presently available from our NMR data, it is the overall similarities between the two molecules, rather than the differences, that are most apparent. Further experimental work, including structural modeling, will be required to refine these structures to the point where the critical differences between them, those which determine their different biological potencies, can be distinguished.

Comparison with Structure of Scorpion Toxins. Scorpions contain a variety of small basic proteins with neurotoxic activity. Amongst these are a series of toxins containing 60–70 amino acid residues, cross-linked by four disulfide bridges, which act by slowing down the inactivation of the sodium channel (Ovchinnikov & Grishin, 1982; Darbon et al., 1985). It appears that the α-scorpion toxins bind to the sodium channel at a site similar to that of ATX II from *Anemonia sulcata* (Couraud et al., 1978), which shares considerable amino acid sequence homology (86%) with AP-A. Thus, although the overall conformations of the scorpion and sea anemone toxins will not necessarily be the same, it is likely that similarities will be found in the regions of these molecules that constitute the site of interaction with the sodium channel.

The X-ray crystal structure of one scorpion toxin, variant 3 from *Centruroides sculpturatus* Ewing, has been determined at high resolution (Fontecilla-Camps et al., 1981). The molecule contains 2.5 turns of α-helix and a short three-strand region of antiparallel β-sheet. The α-helix and β-sheet are linked by two disulfide bridges, with a third located nearby. The backbone defines a large flattened surface that includes the β-sheet and contains a large concentration of hydrophobic residues. Many residues on this surface are conserved throughout the series of scorpion toxins, and it has been suggested by Fontecilla-Camps et al. (1981) that this surface plays a role in the interaction with the sodium channel of excitable membranes, the conserved residues therein possibly being involved in specific interactions with the channel. The variant 3 toxin is a β-toxin, which would be expected to bind to the Na^+ channel at a site distinct from that of the α-toxins and anemone polypeptides (Darbon et al., 1985). Fluorescence studies have shown, however, that both the α- and β-toxin

binding sites are hydrophobic and that they may be conformationally coupled (Darbon & Angelides, 1984).

In AP-A and ATX I, the region of β-sheet contains a number of hydrophobic side chains, and it has been noted above that the aromatic rings of Trp residues 23 and 33 are in close proximity to one another and to other nonpolar side chains. It is possible that this region of these polypeptides could play a similar role in interacting with the sodium channel to that proposed by Fontecilla-Camps et al. (1981) for the "conserved-hydrophobic" surface of the scorpion toxins. Recent photochemically induced dynamic nuclear polarization NMR studies of the environments of aromatic residues in AP-A and ATX I indicate that Trp-23 and -33 are accessible to flavin dye (R. S. Norton, L. Beress, S. Stob, R. Boelens, and R. Kaptein, unpublished results), thus demonstrating that the small hydrophobic cluster involving these two residues is indeed at the surface of these molecules. The region of β-sheet and the interaction between the two Trp residues are present in both AP-A and ATX I. Furthermore, the amino acid substitutions in this region are conservative. The least conservative replacement is that of His-34 in AP-A and ATX II with Asn in ATX I (Beress, 1982), but this residue is on the opposite side of the β-sheet from Trp-23 and -33 and thus points away from the hydrophobic region.

Previously, it has been suggested (Norton et al., 1978, 1980) that a site involving Asp-7 and Asp-9 is involved in the biological actions of AP-A and ATX II. We have shown recently that, while the Asp residues are indeed essential for cardiotonic activity, their modification leads to extensive structural changes in AP-A (Gruen & Norton, 1985). Thus, the role of one or both of these residues may be to maintain the active conformation rather than to interact with the sodium channel directly. Further work is required to identify those residues involved in specific interactions with the sodium channel.

ACKNOWLEDGMENTS

We are indebted to Dr. L. Beress (Department of Toxicology, University of Kiel, FRG) for providing the ATX I used in this study and to Professor T. R. Norton (Department of Pharmacology, University of Hawaii, Honolulu) for providing AP-A used in the initial stages of this work and for his continued interest.

Registry No. AP-A, 60880-63-9.

REFERENCES

Alsen, C. (1983) *Fed. Proc., Fed. Am. Soc. Exp. Biol. 42*, 101–108.

Arseniev, A. S., Kondakov, V. I., Maiorov, V. N., & Bystrov, V. F. (1984) *FEBS Lett. 165*, 57–62.

Aue, W. P., Bartholdi, E., & Ernst, R. R. (1976) *J. Chem. Phys. 64*, 2229–2246.

Beress, L. (1982) *Pure Appl. Chem. 54*, 1981–1994.

Beress, L., Beress, R., & Wunderer, G. (1975) *FEBS Lett. 50*, 311–314.

Bergman, C., Dubois, J. M., Rojas, E., & Rathmayer, W. (1976) *Biochim. Biophys. Acta 455*, 173–184.

Billeter, M., Braun, W., & Wüthrich, K. (1982) *J. Mol. Biol. 155*, 321–346.

Blair, R. W., Peterson, D. F., & Bishop, V. S. (1978) *J. Pharmacol. Exp. Ther. 207*, 271–276.

Braun, W., Bösch, C., Brown, L. R., Gō, N., & Wüthrich, K. (1981) *Biochim. Biophys. Acta 667*, 377–396.

Bystrov, V. F. (1976) *Prog. Nucl. Magn. Reson. Spectrosc. 10*, 41–81.

Chou, P. Y., & Fasman, G. D. (1974) *Biochemistry 13*, 222–245.

Couraud, F., Rochat, H., & Lissitzky, S. (1978) *Biochem. Biophys. Res. Commun. 83*, 1525–1530.

Darbon, H., & Angelides, K. J. (1984) *J. Biol. Chem. 259*, 6074–6084.

Darbon, H., Sampieri, F., El Ayeb, M., & Rochat, H. (1985) *Proceedings of the 16th FEBS Congress*, Part B, pp 423–429, VNU Science Press.

Dufton, M. J., & Hider, R. C. (1977) *J. Mol. Biol. 115*, 177–193.

Fontecilla-Camps, J. C., Almassy, R. J., Ealick, S. E., Suddath, F. L., Watt, D. D., Feldmann, R. J., & Bugg, C. E. (1981) *Trends Biochem. Sci. (Pers. Ed.) 6*, 291–296.

Gooley, P. R., & Norton, R. S. (1985a) *Eur. J. Biochem. 153*, 529–539.

Gooley, P. R., & Norton, R. S. (1985b) *Biopolymers* (in press).

Gooley, P. R., Beress, L., & Norton, R. S. (1984a) *Biochemistry 23*, 2144–2152.

Gooley, P. R., Blunt, J. W., & Norton, R. S. (1984b) *FEBS Lett. 174*, 15–19.

Gooley, P. R., Blunt, J. W., Beress, L., Norton, T. R., & Norton, R. S. (1985) *J. Biol. Chem.* (in press).

Gruen, L. C., & Norton, R. S. (1985) *Biochem. Int. 11*, 69–76.

Havel, T. F., Crippen, G. M., & Kuntz, I. D. (1979) *Biopolymers 18*, 73–81.

Ishizaki, H., McKay, R. H., Norton, T. R., Yasunobu, K. T., Lee, J. & Tu, A. T. (1979) *J. Biol. Chem. 254*, 9651–9656.

Jeener, J., Meier, B. H., Bachmann, P., & Ernst, R. R. (1979) *J. Chem. Phys. 71*, 4546–4553.

Kaptein, R., Zuiderweg, E. R. P., Scheek, R. M., Boelens, R., & van Gunsteren, W. F. (1985) *J. Mol. Biol. 182*, 179–182.

Khaled, M. A., & Urry, D. W. (1976) *Biochem. Biophys. Res. Commun. 70*, 485–491.

Kodama, I., Shibata, S., Toyama, J., & Yamada, K. (1981) *Br. J. Pharmacol. 74*, 29–37.

Nabiullin, A. A., Odinokov, S. E., Kozlovskaya, E. P., & Elyakov, G. B. (1982) *FEBS Lett. 141*, 124–127.

Norton, R. S., & Norton, T. R. (1979) *J. Biol. Chem. 254*, 10220–10226.

Norton, R. S., & Norton, T. R. (1980) in *Frontiers in Protein Chemistry* (Liu, T. Y., Mamiya, G., & Yasunobu, K. T., Eds.) pp 149–156, Elsevier/North-Holland, New York.

Norton, R. S., Zwick, J., & Beress, L. (1980) *Eur. J. Biochem. 113*, 75–83.

Norton, R. S., Norton, T. R., Sleigh, R. W., & Bishop, D. G. (1982) *Arch. Biochem. Biophys. 213*, 87–97.

Norton, T. R. (1981) *Fed. Proc., Fed. Am. Soc. Exp. Biol. 40*, 21–25.

Norton, T. R., Kashiwagi, M., & Shibata, S. (1978) in *Drugs and Food from the Sea, Myth or Reality*? (Kaul, P. N., & Sindermann, C. J., Eds.) pp 37–50, University of Oklahoma Press, Norman, OK.

Ovchinnikov, Yu. A., & Grishin, E. V. (1982) *Trends Biochem. Sci. (Pers. Ed.) 7*, 26–28.

Perkins, S. J. (1982) *Biol. Magn. Reson. 4*, 193–336.

Prescott, B., Thomas, G. J., Beress, L., Wunderer, G., & Tu, A. T. (1976) *FEBS Lett. 64*, 144–147.

Ravens, U. (1976) *Naunyn-Schmiedeberg's Arch. Pharmacol. 296*, 73–78.

Romey, G., Abita, J.-P., Schweitz, H., Wunderer, G., & Lazdunski, M. (1976) *Proc. Natl. Acad. Sci. U.S.A. 73*, 4055–4059.

Scheffler, J.-J., Tsugita, A., Linden, G., Schweitz, H., & Lazdunski, M. (1982) *Biochem. Biophys. Res. Commun. 107*, 272–278.

Schulz, G. E., & Schirmer, R. H. (1979) *Principles of Protein Structure*, Springer-Verlag, New York.
Schweitz, H., Vincent, J.-P., Barhanin, J., Frelin, C., Linden, G., Hugues, M., & Lazdunski, M. (1981) *Biochemistry 20*, 5245-5252.
Scriabine, A., van Arman, C. G., Morgan, G., Morris, A. A., Bennett, C. D., & Bohidar, N. R. (1979) *J. Cardiovasc. Pharmacol. 1*, 571-583.
Shibata, S., Norton, T. R., Izumi, T., Matsuo, T., & Katsuki, S. (1976) *J. Pharmacol. Exp. Ther. 199*, 298-309.
Venkatachalam, C. M. (1968) *Biopolymers 6*, 1425-1436.
Wemmer, D., & Kallenbach, N. R. (1983) *Biochemistry 22*, 1901-1906.
Williamson, M. P., Havel, T. F., & Wüthrich, K. (1985) *J. Mol. Biol. 182*, 295-315.
Wunderer, G., & Eulitz, M. (1978) *Eur. J. Biochem. 89*, 11-17.
Wunderer, G., Fritz, H., Wachter, E., & Machleidt, W. (1976) *Eur. J. Biochem. 68*, 193-198.
Wüthrich, K. (1983) *Biopolymers 22*, 131-138.
Wüthrich, K., Billeter, M., & Braun, W. (1984) *J. Mol. Biol. 180*, 715-740.

Two-Dimensional ^{1}H NMR of Three Spin-Labeled Derivatives of Bovine Pancreatic Trypsin Inhibitor†

Phyllis Anne Kosen, Ruud M. Scheek, Hossein Naderi, Vladimir J. Basus, Sadasivam Manogaran, Paul G. Schmidt,‡ Norman J. Oppenheimer, and Irwin D. Kuntz*

Department of Pharmaceutical Chemistry, University of California, San Francisco, California 94143

Received October 21, 1985; Revised Manuscript Received December 19, 1985

ABSTRACT: Three nitroxide spin-labeled monoderivatives of bovine pancreatic trypsin inhibitor were prepared with the amino-specific reagent succinimidyl 1-oxy-2,2,5,5-tetramethyl-3-pyrroline-3-carboxylate. The monoderivatives were purified by ion-exchange and affinity chromatography. Thin-layer maps of tryptic peptides of the monoderivatives showed that the spin-label was incorporated at either the α-amino group, Lys-15, or Lys-26. Two-dimensional *J*-correlated ^{1}H NMR spectra of the monoderivatives were recorded. Spectra were also recorded after reduction by ascorbic acid of the nitroxide label to hydroxylamine. With the nitroxide label present, significant line-broadening effects on many of the cross peaks in the spectra were observed. The extent of line broadening for the $C_\alpha H$–NH cross peaks was qualitatively correlated with the distance between the labeled amino group and the average $C_\alpha H$–NH position in the crystal structure. The spin-label affects cross peaks of protons within ~15 Å. This study suggests that it is feasible to accumulate sufficient intramolecular distances in order to determine protein solution structures with the aid of distance geometry algorithms.

The advent of high-field two-dimensional NMR[1] spectroscopy has created a renewed interest in obtaining time-averaged solution conformations of macromolecules at a resolution comparable to that of X-ray crystallography. Wüthrich and his colleagues pioneered the combined use of the nuclear Overhauser effect, vicinal coupling constants, and hydrogen exchange rates obtained from two-dimensional spectra to identify regions of secondary structure in proteins (Wagner & Wüthrich, 1982b; Hosur et al., 1983; Pardi et al., 1983; Williamson et al., 1984). As a complementary approach, they have suggested using hydrogen–hydrogen through-space distances obtained from NOESY experiments in conjunction with distance geometry calculations (Havel et al., 1979, 1983; Havel & Wüthrich, 1985) to determine the three-dimensional structure of a protein (Braun et al., 1981, 1983; Wüthrich et al., 1982; Williamson et al., 1985). Others have made a similar suggestion with reference to nucleic acid structure (James et al., 1985). However, as only distances of less than 5 Å can be obtained from NOE studies, the number of distances measured is perhaps an order of magnitude smaller than needed for a medium-resolution protein structure (Havel et al., 1979; Havel & Wüthrich, 1985). Other techniques yielding nonredundant atom to atom distances must be developed to achieve a structure approaching 3-Å resolution.

Recently, reports by two groups have shown that distances between approximately 10 and 20 Å can be extracted from one-dimensional high-resolution NMR data, by incorporating a single nitroxide spin-label into a macromolecule. The distances were found with the distance dependence of the line broadening due to the dipolar relaxation of a given hydrogen by the paramagnetic electron of the spin-label (Solomon & Bloembergen, 1956). Schmidt and Kuntz (1984), repeating

†Supported by Grants GM-19267 (I.D.K.), RR-01695 (I.D.K.), and CA26272 (N.J.O.) from the National Institutes of Health. R.M.S. was supported by a fellowship from the Netherlands Organization for the Advancement of Pure Research (ZWO) and V.J.B. by a grant from the Academic Senate, University of California. The UCSF Magnetic Resonance Laboratory was partially funded by grants from the National Science Foundation (DMB 8406826) and the National Institutes of Health (RR-01668).

‡Present address: Vestar Research Inc., Pasadena, CA 91106.

[1] Abbreviations: NMR, nuclear magnetic resonance; NOESY, two-dimensional nuclear Overhauser enhancement spectroscopy; NOE, nuclear Overhauser enhancement; F_{ab}, N-terminal half of the heavy chain and the whole light chain of immunoglobulin G; COSY, two-dimensional *J*-correlated spectroscopy; BPTI, bovine pancreatic trypsin inhibitor; HPLC, high-performance liquid chromatography; TPCK, L-1-(tosylamido)-2-phenylethyl chloromethyl ketone; CM, carboxymethyl; FPLC, fast-performance liquid chromatography; Tris, tris(hydroxymethyl)-aminomethane; UV, ultraviolet.

0006-2960/86/0425-2356$01.50/0